

53rd SME North American Manufacturing Research Conference (NAMRC 53, 2025)

Design and Fabrication of Biodegradable Bone Tissue Scaffolds Based on the Nuclear Pasta Theory

Hamzeh Al-Qawasmi^a, Roozbeh “Ross” Salary^{a,b*}

^aDepartment of Biomedical Engineering, Marshall University, Huntington, WV 25755, USA

^bDepartment of Mechanical & Industrial Engineering, Marshall University, Huntington, WV 25755, USA

* Corresponding author. Tel.: +1-315-395-4598; fax: +1-304-696-5454. E-mail address: salary@marshall.edu

Abstract

Globally, around 2.2 million bone graft procedures are performed annually, with costs reaching approximately \$664 million as of 2021. The number of surgeries to repair bone defects is projected to increase by about 13% each year. However, traditional bone grafts often carry risks such as donor site morbidity and limited availability, driving the need for innovative solutions. This study explores the fabrication of biodegradable bone tissue scaffolds inspired by the nuclear pasta theory using extrusion-based Fused Deposition Modeling (FDM). The nuclear pasta theory, which describes complex geometrical formations within neutron stars, serves as a novel source of inspiration for designing scaffolds with enhanced mechanical properties and optimized porosity. Two bio-based, biodegradable polymers, Luminy LX175 and ecoPLAS, were used to fabricate scaffolds via an in-house filament extrusion process utilizing the Filabot EX6 system. The extrusion parameters were optimized to achieve a consistent filament diameter of 1.75 mm suitable for 3D printing on a Creality K1C printer. Seven scaffold designs were developed, including five based on Triply Periodic Minimal Surfaces (TPMS) and two inspired by nuclear pasta configurations, namely "lasagna" and a hybrid "lasagna-spaghetti" structure. The scaffolds were evaluated for their mechanical properties using uniaxial compression testing. Results showed that TPMS-inspired designs generally achieved a favorable balance between porosity and mechanical strength, while the nuclear pasta-inspired designs exhibited unique anisotropic and isotropic compression characteristics. The study concluded that nuclear pasta-inspired scaffold architectures exhibit unique mechanical properties and porosity characteristics, emphasizing their potential for future optimization in bone tissue engineering applications. Additionally, these structures can be further reinforced through material modifications or hybrid scaffold designs to enhance their load-bearing capabilities. This work demonstrates the potential of using bio-inspired designs in conjunction with sustainable, biodegradable materials for bone tissue engineering. Future research will focus on optimizing co-extrusion techniques and exploring composite materials to further enhance scaffold properties for clinical applications.

© 2025 The Authors. Published by ELSEVIER Ltd. This is an open access article under the CC BY-NC-ND license (<https://creativecommons.org/licenses/by-nc-nd/4.0>)

Peer-review under responsibility of the scientific committee of the NAMRI/SME.

Keywords: Regenerative Medicine; Bone Tissue Engineering; 3D Biofabrication; Scaffold Design; Nuclear Pasta

1. Introduction

1.1. Background

Additive manufacturing, particularly using extrusion-based Fused Deposition Modeling (FDM) 3D printing, has emerged as a versatile and powerful tool for fabricating custom scaffolds with complex geometries, making it a highly effective approach for tissue engineering applications [1]. The ability to design scaffolds that replicate the structure and mechanical properties

of trabecular bone, particularly in load-bearing regions such as the femur and tibia, is crucial for promoting bone regeneration and repair [2-5]. These scaffolds must not only support cellular growth and nutrient transport but also provide sufficient mechanical strength and biocompatibility to facilitate effective tissue repair [6]. The development and use of biodegradable polymers further enhances the potential of 3D-printed scaffolds, enabling the creation of structures that naturally degrade as new bone tissue forms, thus reducing the need for secondary surgical procedures.

The nuclear pasta theory describes a series of complex structures theorized to exist within the crusts of neutron stars. These structures, formed under extreme pressures and densities following a supernova event, exhibit geometries resembling various shapes of pasta, such as sheets ("lasagna"), tubes ("spaghetti"), and more intricate formations. These configurations arise from the competition between nuclear attraction and Coulomb repulsion forces, leading to energy-minimizing structures [7].

In the context of bone tissue engineering, the complexity and periodic geometries of nuclear pasta structures can inspire scaffold designs that mimic the porous architecture of natural bone. Nuclear pasta geometries offer several distinct properties that could theoretically enhance scaffold performance. These include high internal porosity, which facilitates cell infiltration and nutrient flow, as well as an interconnected structure that mimics the extracellular matrix, supporting cellular activity in future studies. Additionally, these geometries exhibit both anisotropic and isotropic mechanical characteristics, allowing for directional strength in specific areas or uniform strength across the entire scaffold. These properties not only make nuclear pasta-inspired designs well-suited for balancing mechanical strength with adequate porosity, but they also open the door to exploring nontraditional scaffold designs in future analyses. While the nuclear pasta-inspired scaffold designs incorporate intricate geometries, their selection was driven by their structural efficiency and potential to enhance mechanical performance and porosity, both critical factors in bone tissue engineering. Effective porosity is needed for material transport, facilitating the delivery of oxygen, nutrients, and growth factors necessary for cell proliferation and tissue development. Similar bioinspired geometries, such as triply periodic minimal surfaces models [8-10], have already demonstrated success in biomedical research for clinical applications. Such designs aim to optimize mechanical strength while facilitating cell infiltration and nutrient flow, both of which are crucial for effective bone regeneration. By emulating these natural formations, scaffolds can achieve an optimal balance between porosity and mechanical integrity, thus promoting better integration with host tissue.

Systematically assessing the numerous parameters in scaffold parametric design, such as pore size, wall thickness, and overall geometry, requires a structured approach that combines experimental testing with computational modeling. One effective method is to use design of experiments (DOE) or machine learning techniques to explore a wide range of parameter combinations while systematically varying key factors to assess their impact on scaffold performance. Finite element analysis (FEA) and other computational tools can also be employed to predict mechanical and biological behavior across different design variations, enabling the identification of optimal configurations. The exploration of new options should reasonably stop when a set of design parameters consistently meets the performance criteria, such as mechanical strength, porosity, and biocompatibility, without introducing diminishing returns in terms of additional complexity or manufacturing difficulty. Further exploration would then focus on refining the selected parameters rather than continuously expanding the design space.

1.2. Objective of the Study

The primary objective of this study was to assess the feasibility of fabricating nuclear pasta phase-inspired bone tissue scaffolds through an in-house filament extrusion process using eco-friendly, bio-based polymers. This research utilized the Filabot EX6 extrusion system to produce high-quality filaments from two biodegradable materials, LX175 and ecoPLAS, and evaluated their suitability for 3D printing applications. These materials were specifically chosen for their sustainable and biocompatible properties, making them ideal candidates for biomedical applications.

By utilizing the Filabot EX6 system, a high degree of control over filament diameter and consistency was achieved, which is critical for ensuring the printability and reproducibility of scaffolds. Consistent filament quality is essential for maintaining the structural integrity of the printed scaffolds, as even minor deviations in diameter can negatively impact their mechanical properties. While this study focused on single-material filament production, it also lays the groundwork for future explorations into co-extrusion of multiple materials to enhance scaffold performance. Future research may investigate combining different polymers to optimize mechanical properties, such as stiffness and compressive strength, while fine-tuning degradation rates to align with bone healing processes.

In addition to filament fabrication, this study also explored the use of advanced scaffold designs to enhance the mechanical and biological performance of the printed structures. Five Triply Periodic Minimal Surface (TPMS) designs [1] and two nuclear pasta-inspired scaffolds were selected for their potential to replicate the intricate porous structure of natural bone matrix. TPMS geometries are known for their optimal balance between strength and porosity, which is crucial for bone tissue regeneration. Meanwhile, the nuclear pasta designs, inspired by the dense arrangements found in neutron star matter, introduce a novel approach to scaffold architecture, potentially improving mechanical stability and tissue integration.

1.3. Literature Review

The incorporation of TPMS geometries in scaffold designs has been extensively studied due to their ability to optimize mass transport, reduce stress shielding, and enhance the mechanical properties of scaffolds. TPMS-based scaffolds offer a favorable bath and porosity [11], creating an ideal microenvironment for osteocyte proliferation. Studies have demonstrated that TPMS structures can be optimized for fluid characteristics and graded mechanical properties, making them versatile for bone tissue engineering.

The mechanical properties of scaffolds, particularly compression modulus of elasticity, are crucial for their use in bone tissue engineering. These properties must align with the mechanical characteristics of native bone to support load-bearing during the healing process and to facilitate tissue regeneration. Gerhardt *et al.* [12] demonstrate that native bone exhibits considerable variability in compression modulus, with

trabecular bone ranging from 0.12 to 1.1 GPa and cortical bone from 11.5 to 17 GPa.

Jiang *et al.* [13] present a novel approach to designing TPMS-based bone scaffolds aimed at improving biological and mechanical performance. By introducing optimization-guided multi-functional pores, the study achieves a coordination between structural integrity and biological efficacy.

Depeng *et al.* [14] investigate functionally graded TPMS scaffolds, focusing on optimizing stress distribution and mass transport. The study uses finite element analysis to demonstrate how these designs can enhance both mechanical strength and permeability, crucial for effective bone regeneration.

Homavand *et al.* [15] explore the reinforcement of polylactic acid with eggshell-derived calcium carbonate particles to enhance its mechanical properties. The study highlights the potential of using natural fillers like eggshells to improve the tensile strength and rigidity of PLA composites.

Caplan *et al.* [16] discuss the unique properties of materials in astronomical objects, focusing on the elasticity of nuclear pasta. This study examines the properties and breaking mechanisms of nuclear pasta structures in neutron star crusts using simulations to determine their potential strength.

Xia *et al.* [17] examine the relationship between nuclear pasta structures and the symmetry energy in neutron stars, providing insights into the equation of state of dense matter. The study employs relativistic mean-field models to analyze these phenomena.

Li [7] reviews the use of classical molecular dynamics simulations to study the morphological and thermodynamic properties of nuclear pasta, providing a comprehensive overview of recent advancements in the field.

While previously mentioned studies have focused on optimizing TPMS scaffold designs, enhancing mechanical properties, and reinforcing PLA composites, they have not explored the integration of nuclear pasta-inspired geometries into scaffold design. This study addresses this gap by leveraging the unique structural configurations of nuclear pasta to develop bone scaffolds while performing a thorough feasibility analysis. Unlike conventional TPMS or reinforced composites, the nuclear pasta-inspired designs aim to optimize anisotropic and isotropic mechanical properties, providing a novel approach to enhancing tissue integration and load-bearing capabilities in bone scaffolds. This innovative approach combines insights from astrophysics with scaffold engineering to push the boundaries of what is achievable in bone tissue regeneration.

In this study, Sec. 2 provides a detailed overview of the materials and methods utilized, while Sec. 3 presents the results, along with a comparative analysis of material properties in Sec. 4. Lastly, Sec. 5 outlines the conclusions and potential directions for future research.

2. Material and Methodology

2.1. Materials

Two biodegradable polymers were selected for scaffold fabrication, including Luminy LX175 (TotalEnergies Corbion, Gorinchem, Netherlands), and ecoPLAS 3D201 (Filabot, Barre,

VT). LX175 is a PLA-based material, specifically known for its high viscosity and low flow properties, which are essential for creating filaments with consistent diameter. It is derived from renewable resources, making it both sustainable and non-toxic, suitable for biomedical applications. Additionally, ecoPLAS is a composite material that combines polylactic acid (PLA) with calcium carbonate (CaCO_3) derived from limestone, providing increased stiffness and rigidity compared to unfilled PLA. This material was chosen for its ability to sequester carbon dioxide (CO_2) throughout its lifecycle, further enhancing its sustainability profile. Both materials were deemed compatible with the extrusion setup in accordance with the safety and technical datasheets provided by the manufacturer for both materials, which was crucial for producing quality filaments which were capable of being printed efficiently.

2.2. Filament Extrusion Process

The filament extrusion process was conducted using the Filabot EX6 single-screw extrusion system, selected for its control over extrusion parameters necessary for producing filaments with a consistent and compatible target diameter of 1.75 mm. Achieving this precision is essential to ensure the reliability and reproducibility of the subsequent 3D printing phase of the study [1].

This system is composed of several integrated components, each playing a determining role in ensuring the production of high-quality filaments. The components are as follows in chronological order of usage: (i) Filabot EX6 Extruder, (ii) Filabot Airpath, (iii) Filabot Spooler, (iv) Filameasure Inline, (v) Filament Measurement System, (vi) Filalogger Software.

Once the pellets enter the extruder via the mounted hopper, the EX6 extruder precisely controls the heating and extrusion process. The extruder is divided into four separate heating control zones, allowing for independent temperature control along the barrel. For this study, the extrusion of LX175 and ecoPLAS was conducted with optimized middle heat zone temperatures of 166 °C for LX175 and 164 °C for ecoPLAS. This adjustment was based on our experimental observations aimed at achieving optimal filament quality, particularly for bone tissue scaffold applications.

By fine-tuning the middle heat zone to 164–166 °C, the risk of thermal degradation was reduced while maintaining consistent material flow. This adjustment was critical for producing filaments with the uniformity required for reliable 3D printing, ensuring that the mechanical properties of the final constructs would not be compromised. Additionally, optimizing this temperature range helped preserve the biocompatibility of the materials, which is essential for their intended use in tissue engineering. The experimental extrusion, cooling, and winding setup is displayed in Figure 1.

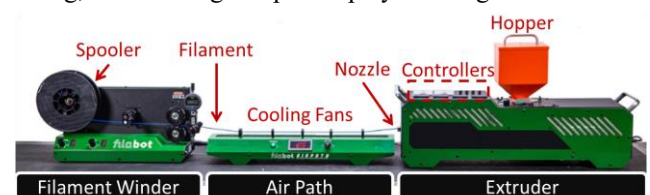


Figure 1. Filament extruder, airpath, and winder setup.

Additionally, the complete extrusion parameters are displayed in Table 1, as follows:

Table 1. Extrusion parameters visualized, including drive speed, heat zone temperatures, and fans.

Extrusion Parameter	Value	Unit
Extrusion Speed Voltage	10	Volts (V)
Extrusion Speed Amperage	1.2-1.3	Amperes (A)
Feed Temperature	40.0	°C
Back Temperature	163.3-165.0	°C
Middle Temperature	164.3-166.0	°C
Front Temperature	165.8-167.0	°C
Motor Fan	Full	(Dial)
Feed Fan	Half	(Dial)
Back Fan	N/A	(Dial)
Middle Fan	Half	(Dial)
Front Fan	Half	(Dial)

As the filament exits the extruder, it is first directed through a controlled cooling path to solidify and stabilize its shape. The cooling system gradually reduces the filament's temperature to prevent warping or internal stresses that could affect its mechanical properties. This controlled cooling is particularly important for biodegradable polymers like LX175 and ecoPLAS, which are sensitive to abrupt temperature fluctuations.

After cooling, the filament passes through an inline filament diameter measurement system (Mitutoyo Filameasure), which is mounted directly on the spooler. This system continuously measures the filament diameter as it is being wound onto the spool, ensuring that the cooled filament maintains the target diameter of 1.75 mm. By measuring the diameter at this final stage, any deviations that may occur post-cooling can be detected and addressed immediately. This setup ensures that the filament maintains its uniformity, which is critical for reliable 3D printing performance.

The Filobot Spooler operates at a controlled speed to prevent excess tension, which could cause deformation of the filament. With an increased spool drive and low extrusion speed, the filament experiences thinning, which results in a decreased diameter. Conversely, a decreased spool drive and high extrusion speed exhibits an increase in filament diameter. It is necessary to continually monitor the drive speeds on both components to ensure a stable flow and adequate diameter for further analysis. Maintaining consistent spooling is pivotal for preserving the structural integrity of the filament throughout its length.

During the extrusion process, the Filallogger software graphically displays the filament diameter in real-time and also stores detailed numerical data for historical analysis. This data logging capability allows for continuous monitoring of diameter consistency during extrusion. The stored data can be reviewed to identify trends, optimize future extrusion settings, and ensure that the filament remains within the specified tolerance range. This combination of real-time graphical display and historical data storage provides a robust quality

control mechanism, enabling the production of consistent, high-quality filaments tailored for clinical applications.

2.3. Scaffold Design and CAD Modeling

In this study, a labeling system was implemented to allow for efficient categorization of the various scaffold samples ensuring clarity and consistency throughout the study duration. The samples were given the structure M-D-R, where M denotes the material used (with M1 representing Luminy LX175 and M2 for ecoPLAS), D represents the design number (ranging from D1 to D7 for the various scaffold geometries), and R refers to the replicate number (e.g., R1 to R6 for multiple iterations of each design). This labeling system was crucial for organizing and categorizing the large dataset generated during experimentation to optimize efficiency and allowing for systematic analysis of how material type, scaffold design, and replication influence mechanical properties and performance.

Overall, two materials (M1-M2) and seven designs (D1-D7) were studied. Each sample was replicated six times (R1-R6), resulting in a total of 84 scaffold samples. R6 was kept aside and designated for future cellular analysis on the proliferation and adhesion of osteocytes from mesenchymal stem cells. Please note that the scaffolds are designed for the regeneration of both trabecular and cancellous bone in load-bearing sites such as the femur and tibia. Designed to be bioresorbable, they also aim to facilitate a controlled, gradual degradation process, ensuring seamless integration with native bone tissue while supporting long-term structural integrity.

Indiana University's Advanced Visualization Lab provided the nuclear pasta 3D models used in this research [18]. These models were adapted and optimized for scaffold fabrication via Autodesk Meshmixer, demonstrating the potential of using astrophysical geometries to inspire innovative biomedical designs. Samples containing D1-D5 were based on TPMS equations, modified using Rhinoceros 3D and Grasshopper to develop their structural properties. Figure 2 displays an overhead view of the 3D models following its creation in CAD, prior to the fabrication process.

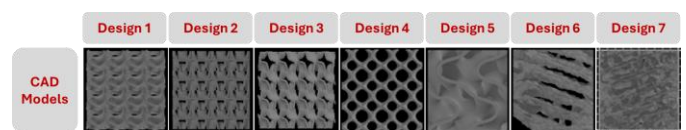


Figure 2. CAD models of D1-7 from an overhead perspective, using 3D Viewer.

D6 and D7 were inspired by the dense configurations found in nuclear pasta structures, with the "Lasagna" design (D6) tailored for anisotropic compression strength and the "Lasagna-Spaghetti" hybrid (D7) intended to enhance isotropic mechanical performance [19]. The CAD models were optimized to ensure printability while maintaining the desired pore architecture, key for cell proliferation and nutrient flow. The incorporation of anisotropic features via the Lasagna architecture into a hybrid scaffold (composed of both Lasagna and Spaghetti designs) served as a reinforcement strategy for nuclear pasta structures that otherwise faced printability challenges. Notably, the original Spaghetti design alone was

deemed unprintable; however, the incorporation of the Lasagna architecture helped uphold the overall scaffold integrity, as exhibited. This strategy enhances the structural performance of scaffolds intended for bone tissue engineering applications.

A systematic approach was utilized when adjusting several parameters that could affect scaffold performance. In our study, key design variables such as pore size, wall thickness, and overall geometry were regulated by both Rhinoceros 3D and Creality Print. Further adjustments were made in the Creality Print slicer to fine-tune parameters such as wall thickness and layer height and ensure that the printed scaffolds accurately replicated the intended CAD designs. This iterative process enabled us to assess the impact of design modifications on mechanical properties, porosity, and overall scaffold performance. Additionally, while there were many possible avenues for further exploration, our focus shifted to evaluating the scaffold designs' key performance indicators until we reached a state that we anticipated would meet the needs of the application upon refinement.

2.4. 3D Printing of Scaffolds

The extruded filaments were used to print scaffolds on a Creality K1C 3D printer, selected for its high-resolution capabilities, reliable performance, and unicorn tri-metal nozzle for increased thermal conductivity, wear resistance, and heat break performance. The printing setup is exhibited in Figure 3. Print settings were carefully adjusted to achieve an optimal balance between mechanical strength and porosity, essential for bone tissue scaffold applications [20]. The layer height was set to 0.2 mm, while the nozzle width was configured to 0.4 mm.

To ensure optimal layer adhesion, the nozzle temperature was set to 200 °C for both LX175 and ecoPLAS filaments. The print speed was maintained at 50 mm/s to ensure consistent material flow and minimize the risk of defects. The seam position was aligned to reduce visible layer lines, and no supports or brims were used, allowing for clean and precise prints.

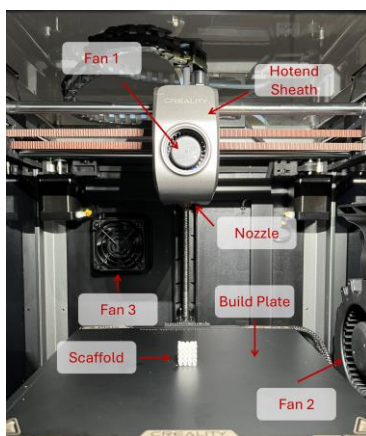


Figure 3. 3D printer overview showcasing notable components and fabrication process.

Each scaffold was printed with these consistent settings, as shown in Table 2, to reduce variability and ensure reproducibility across samples. Figure 4 characterizes the results following the end of the fabrication process, with the

completed scaffolds photographed for documentation and image analysis. Quality control was enforced by visually inspecting each print for defects and verifying dimensions using a digital caliper.

Table 2. Printing parameter protocol followed over the duration of the study.

Printing Parameter	Value
Target model dimensions	15×15×15 mm
Nozzle width	0.4 mm
Layer height	0.2 mm
Printing temperature	200 °C
Bed temperature	50 °C
Fan speed	100%
Print speed	50 mm/s
Seam position	Aligned
Supports	None
Brim/Skirt	None

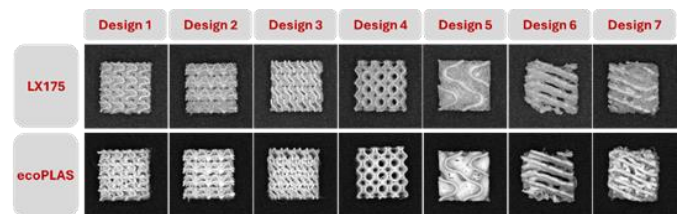


Figure 4. Resulting scaffolds following 3D printing with both materials shown.

2.5. Mechanical Characterization

The mechanical properties of the printed scaffolds were evaluated through uniaxial compression testing using an MTI-10K compression testing machine. Each scaffold sample was subjected to a gradually increasing load, applied at a rate of 0.08 mm/s, until failure occurred. Stress-strain data were collected, and the compression modulus was calculated to assess the stiffness of each scaffold design. The goal was to identify which design and material combination provided the optimal point required for sufficient pore fabrication in these models to ensure a channel network throughout the structure. Additionally, the ability to handle a compressive load is mandatory to construct a clinically feasible bone tissue scaffold. MATLAB was used for data analysis, extracting the slope of the linear region of the stress-strain curves to determine the elastic region. These tests provided insights into the mechanical robustness of each scaffold, essential for biomedical engineering applications.

3. Results and Discussion

3.1. Deposition Mass Analysis

For this study, deposition mass represents the amount of material extruded and deposited onto the build plate during the 3D printing process for each scaffold design (D1–D7). The results indicate a relatively consistent deposition mass across most designs, with a slight increase observed in D2 and D7. D1

exhibited the lowest deposition mass, which may be attributed to variations in filament flow or the geometric complexity and printability challenges of the design.

Maintaining consistent deposition mass across different designs is crucial for ensuring uniformity in scaffold structure, which directly influences mechanical properties. However, even slight variations can impact scaffold density and porosity, which are critical factors in tissue engineering applications. Ensuring consistent deposition mass is essential for achieving reproducible results, particularly when optimizing the mechanical and biological performance of scaffolds for clinical applications. Figure 5 presents these values.

The deposition mass of the scaffolds provides insight into material flow characteristics and printability. Both LX175 and ecoPLAS exhibited consistent deposition across most designs, though differences in viscosity and material composition resulted in variations in mass distribution.

During scaffold fabrication, material #2 (M2, i.e., ecoPLAS) exhibited excellent flow characteristics throughout the printing process. While stringing was observed, no structural deformities were noted. However, the higher viscosity of M2 resulted in more consistent extrusion, particularly for complex designs. The presence of CaCO_3 in ecoPLAS contributes to increased stiffness, allowing for efficient material deposition without compromising printability. Figure 6 presents the deposition mass results.

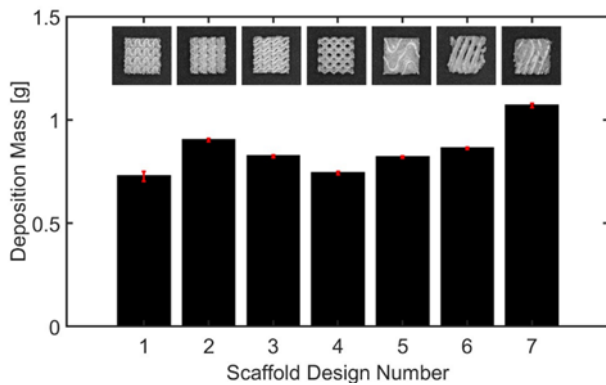


Figure 5. Deposition mass per scaffold design for material #1 (M1), i.e., LX175.

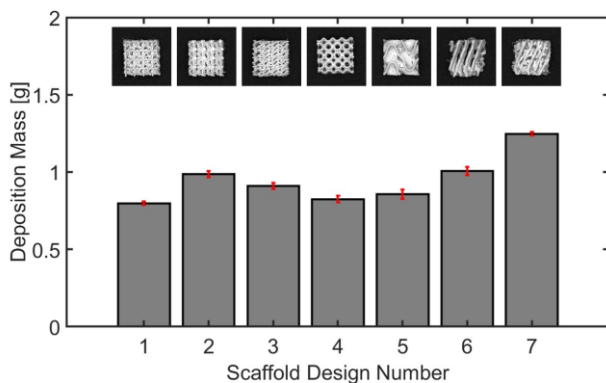


Figure 6. Deposition mass per scaffold design for material #2 (M2), i.e., ecoPLAS.

3.2. Density Analysis

The density measurements of each design under material #1 (M1, i.e., LX175) and material #2 (M2, i.e., ecoPLAS) are presented in Figure 7 and Figure 8, respectively. Density is a key factor in determining a scaffold's mechanical properties and its capacity to support cellular infiltration and nutrient flow through its porous structure. The results reveal that D2 exhibited the highest density, while D1 had the lowest. The relatively higher density of D2 may contribute to its enhanced mechanical properties, as observed in subsequent compression testing.

Variations in density among the designs can be linked to differences in porosity and internal architecture, which directly influence the scaffold's ability to mimic the mechanical behavior of natural bone. Typically, higher-density designs are expected to demonstrate greater compressive strength; however, this may come at the cost of reduced porosity, which is essential for effective tissue integration and nutrient diffusion.

Density plays an important role in scaffold performance, affecting both mechanical strength and porosity. The results indicate that ecoPLAS scaffolds generally exhibited higher density due to the presence of CaCO_3 , while LX175 maintained a lower density, which may enhance cell infiltration.

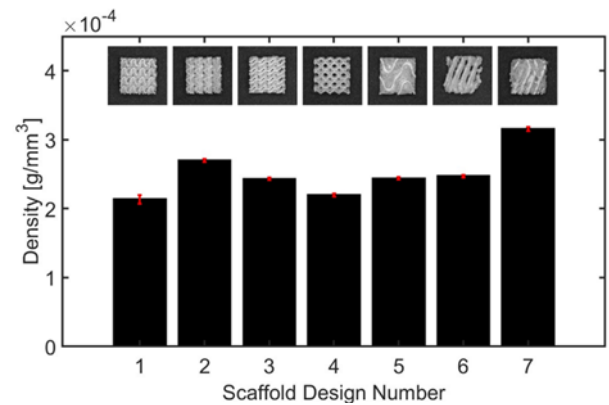


Figure 7. Density per scaffold design for material #1 (M1), i.e., LX175.

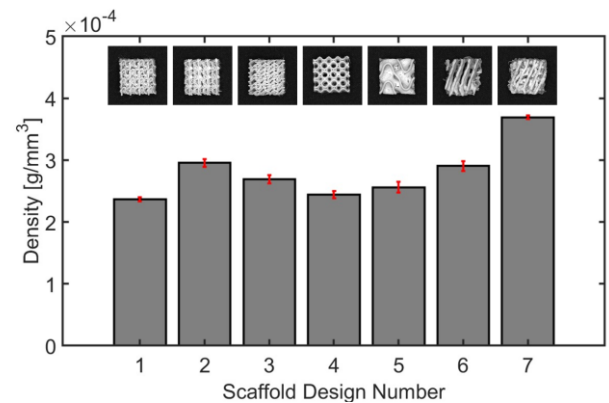


Figure 8. Density per scaffold design for material #2 (M2), i.e., ecoPLAS.

The density results, shown in Figure 8, indicate that ecoPLAS scaffolds generally exhibited higher density across

the various designs. D7 had the highest density, while D1 exhibited the lowest. The CaCO_3 filler in ecoPLAS increases its overall density, leading to a more compact structure.

The higher density in ecoPLAS scaffolds is advantageous for applications where mechanical robustness is required. However, increased density may reduce scaffold porosity, which is essential for effective nutrient flow and cellular infiltration.

3.3. Compression Modulus Analysis

The compression modulus, commonly known as Young's modulus, is an indicator of the scaffolds' stiffness, reflecting their ability to withstand compressive forces without deformation. The compression data for M1 is shown in Figure 9.

Among the designs, D5 exhibited the highest compression modulus, indicating superior mechanical strength compared to the other designs. In contrast, D1 displayed the lowest compression modulus, likely due to its lower density and deposition mass, factors that contributed to reduced mechanical performance.

While D6 and D7 demonstrated moderate compression modulus values, their performance differed significantly due to their distinct structural characteristics. The sheet-like, anisotropic structure of D6 was designed to provide directional strength along the Y-axis while sacrificing stiffness along the X-axis. This resulted in greater variability in the compression modulus, with D6 showing a larger margin of error compared to other designs. The uneven distribution of compressive forces across the scaffold, coupled with a rougher surface finish from the K1C printer, likely contributed to this variability. Consequently, D6 exhibited the second-lowest compression modulus, suggesting that while it provided adequate porosity for cell infiltration, it struggled to maintain consistent load-bearing capacity.

In contrast, D7 was engineered to balance the anisotropic properties of the "lasagna" structure with the isotropic strength provided by the "spaghetti" elements. This hybrid design resulted in a more uniform distribution of compressive forces, enhancing the scaffold's overall mechanical stability. As a result, D7 exhibited a higher compression modulus than D6, demonstrating improved load-bearing capabilities while maintaining sufficient porosity for tissue integration. The combination of sheet-like layers with interconnected strands provided a synergistic effect, making D7 more resilient under compressive stress.

The compression modulus for ecoPLAS scaffolds is presented in Figure 10. The modulus output varied across different designs. D5 exhibited the highest compression modulus, suggesting increased mechanical strength. In contrast, D6, with its "lasagna" configuration, showed the lowest modulus, likely due to its anisotropic structure, which distributes compressive forces unevenly.

The unique composition of ecoPLAS contributes to its moderate stiffness, due to the addition of CaCO_3 . However, the results show that the stiffness achieved is still lower than that of pure PLA materials like LX175. D7, which incorporates both "lasagna" and "spaghetti" configurations, demonstrated a

moderate modulus value, suggesting that the hybrid design improves mechanical performance by distributing compressive forces more evenly, compared to the purely anisotropic nature of D6.

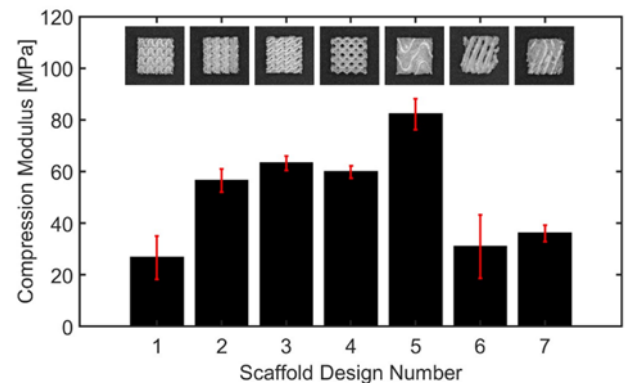


Figure 9. Compression modulus per design for material #1 (M1), i.e., LX175.

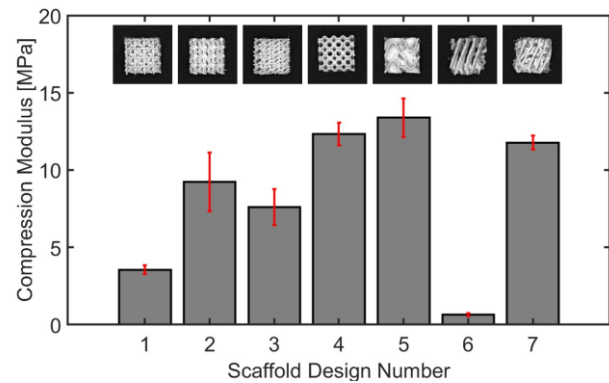


Figure 10. Compression modulus per scaffold design for material #2 (M2), i.e., ecoPLAS.

An analysis of variance (ANOVA) was conducted to assess the variance in deposition mass, density, and Young's modulus across the seven scaffold designs for the two materials. It was observed that scaffold design had a statistically significant effect on the deposition mass (observed for LX175 and ecoPLAS, respectively having a p -value of $2.48\text{E-}21$ and $5.18\text{E-}16$). A statistically significant difference was also observed in density, with LX175 and ecoPLAS yielding p -values of $6.82\text{E-}22$ and $1.04\text{E-}15$, respectively, highlighting the impact of design on scaffold compactness. Furthermore, differences in Young's modulus of elasticity were statistically significant, with p -values of $1.08\text{E-}05$ for LX175 and $9.94\text{E-}07$ for ecoPLAS, indicating that scaffold design substantially influences mechanical stiffness.

4. Comparative Analysis of Material Properties

4.1. Material Influence on Compression Modulus

The compression modulus results highlight that LX175 generally achieved higher stiffness across most designs due to its homogeneous PLA structure, which supports effective load

distribution. In TPMS-based designs like D5, LX175 excelled in stiffness, making it suitable for load-bearing applications.

On the other hand, ecoPLAS, which incorporates CaCO_3 , resulted in higher densities but lower stiffness compared to M1. The increased density of M2 benefits structural compactness but compromises stiffness, as seen in designs like D6. However, the material's flow properties allowed for adequate deposition, especially in complex designs like D7. A frame-by-frame analysis was conducted to obtain photos during compression, featured in Figure 11 and Figure 12.

4.2. Compression Modulus Across Designs

LX175 exhibited superior compression modulus values in D1–D5 due to its ability to distribute loads more effectively. In contrast, ecoPLAS, while achieving higher density, demonstrated lower modulus values, suggesting a balance between density and stiffness.

The performance gap between the two materials was most evident in D6 and D7. For Material 1, D6 and D7 demonstrated similar results in terms of Young's modulus, with values of 30.9 MPa and 36.1 MPa, respectively. In contrast, for Material 2, D6 exhibited a notably low mean compression modulus of 0.646 MPa, while D7 achieved a significantly higher value of 11.8 MPa. The anisotropic structure of D6 led to low stiffness in ecoPLAS due to uneven force distribution, whereas the hybrid design of D7 allowed ecoPLAS to better balance strength and porosity.

To further illustrate these differences, Figure 11 and Figure 12 provide visual evidence of the deformation behavior of each scaffold material under compression testing. These images reveal how LX175 scaffolds maintained a more structured failure pattern, while ecoPLAS samples exhibited greater localized deformation due to the material composition, likely from the addition of CaCO_3 . The visual comparison underscores LX175's greater load-bearing capacity and structural integrity under compressive stress. Additionally, D6's anisotropic structure contributed to uneven force distribution, which is evident in the deformation patterns observed in Figure 12.

Overall, Figure 11 and Figure 12 help contextualize the observed differences in mechanical behavior. LX175 outperformed ecoPLAS in both D6 and D7, reinforcing its greater suitability for applications that demand higher stiffness and structural integrity.

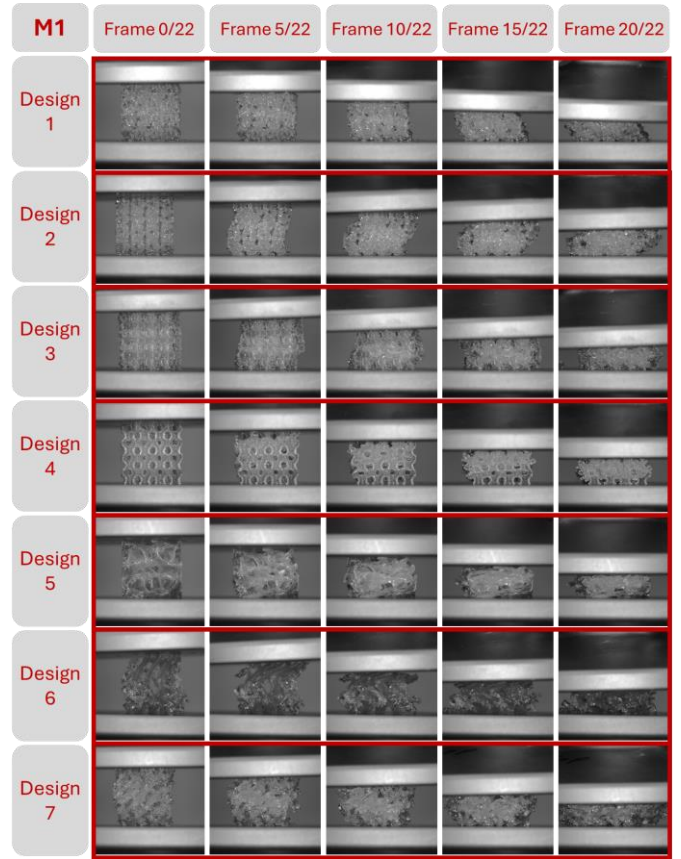


Figure 11. Deposition mass per scaffold design for M1.

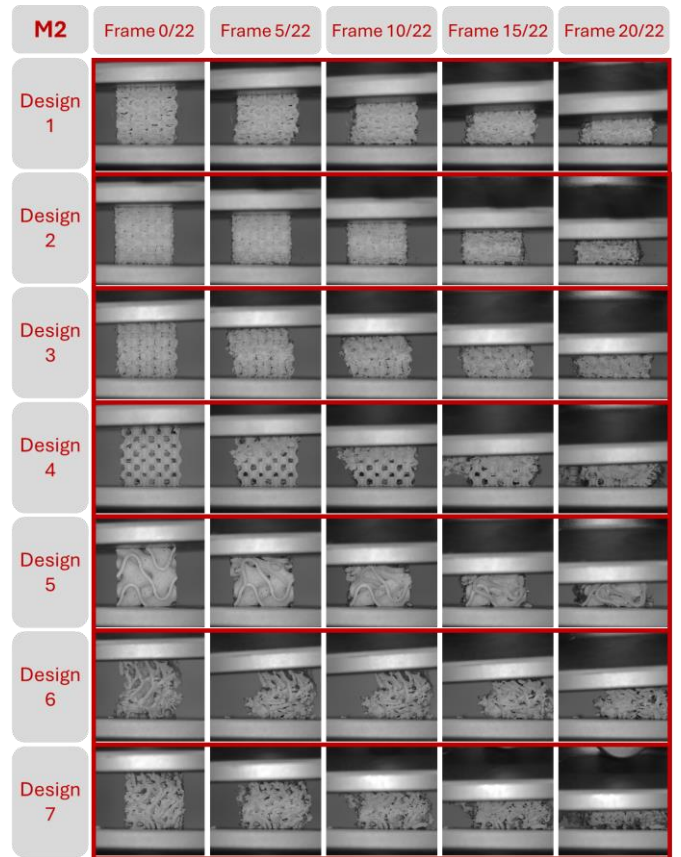


Figure 12. Deposition mass per scaffold design for M2.

4.3. Benchmark Comparison of Compression Modulus

Among the scaffold designs, Design 5 composed of LX175 exhibited the highest compression modulus, with a mean value at 82.12 MPa, making it the most mechanically robust structure in this study. While this value remains slightly below the range of natural trabecular bone (0.12-1.1 GPa) [12], it aligns with expectations for biodegradable scaffolds that prioritize porosity and biointegration over direct load-bearing through further fine-tuning. The combination of structural integrity and controlled porosity in D5-M2 highlight its potential for applications requiring enhanced mechanical stability. To address this, future work will explore material reinforcements, such as ceramic or hydroxyapatite composites, to further optimize scaffold performance suitable for bone tissue engineering.

5. Conclusions and Future Work

This study investigated the design, fabrication, and mechanical characterization of bone tissue scaffolds using two biodegradable materials: Luminy LX175 and ecoPLAS 3D201. By leveraging advanced scaffold designs, including scaffolds fabricated driven by nuclear pasta-inspired configurations and TPMS-based structures, the research aimed to optimize scaffold performance for bone tissue engineering applications. The results demonstrated that material properties significantly influence scaffold performance.

LX175 (M1), a pure PLA-based material, exhibited both increased stiffness and better flow characteristics compared to ecoPLAS, leading to more consistent deposition across various designs. Its homogeneous structure supports efficient load distribution, making it highly suitable for load-bearing applications. Additionally, its excellent flow properties contributed to more uniform filament extrusion, reducing defects during printing. The superior flow properties and mechanical strength in this material makes it more suitable for applications that require consistent deposition and high stiffness. Contrastingly, ecoPLAS, while beneficial for increased density, showed variability in flow, which may have affected the print quality in these complex designs.

The TPMS designs outperformed nuclear pasta-inspired configurations in terms of mechanical robustness, while nuclear pasta designs such as D7 exhibited potential for balancing the mechanical strength with porosity, which is crucial for bone tissue regeneration.

Achieving a balance between stiffness and porosity is vital for effective tissue scaffolding. This study indicates that optimizing both material choice and scaffold geometry can lead to improved scaffold performance tailored to specific clinical needs. While this study primarily focused on scaffold fabrication and mechanical characterization, future research will explore cellular interactions, including osteoblast proliferation and adhesion, to further validate the biocompatibility and effectiveness of these structures for bone tissue engineering applications.

The second material, ecoPLAS (M2), a composite of PLA and CaCO₃, achieved higher densities but exhibited less consistent flow, particularly in complex designs. The addition

of CaCO₃ enhanced its overall stiffness and density but did not match the flow smoothness of LX175. The moderate compression modulus and occasional extrusion inconsistencies suggest that ecoPLAS requires further optimization for high-precision applications.

Acknowledgements

Dr. Salary would like to thank the National Science Foundation (NSF) for funding this work under award # OIA-2327460 as well as the National Aeronautics and Space Administration (NASA) under award # 80NSSC24K0607.

References

- [1] Al-Qawasmi, H., Risch, S., and Salary, R. R., "Polypropylene and Glass Fiber Composite Extrusion for Additive Biofabrication of Bone Tissue Scaffolds With Complex Microstructures," Proc. International Manufacturing Science and Engineering Conference, MSEC2024-123879, V001T03A003; 9 pages, American Society of Mechanical Engineers, DOI: 10.1115/MSEC2024-123879.
- [2] Alonzo, M., Primo, F. A., Kumar, S. A., Mudloff, J. A., Dominguez, E., Fregoso, G., Ortiz, N., Weiss, W. M., and Joddar, B., 2021, "Bone Tissue Engineering Techniques, Advances, and Scaffolds for Treatment of Bone Defects," *Current opinion in biomedical engineering*, 17, p. 100248, DOI: 10.1016/j.cobme.2020.100248.
- [3] Bose, S., Vahabzadeh, S., and Bandyopadhyay, A., 2013, "Bone Tissue Engineering Using 3D Printing," *Materials today*, 16(12), pp. 496-504, DOI: 10.1016/j.mattod.2013.11.017.
- [4] Feng, P., Wu, P., Gao, C., Yang, Y., Guo, W., Yang, W., and Shuai, C., 2018, "A Multimaterial Scaffold with Tunable Properties: Toward Bone Tissue Repair," *Advanced science*, 5(6), p. 1700817, DOI: 10.1002/advs.201700817.
- [5] Orciani, M., Fini, M., Di Primio, R., and Mattioli-Belmonte, M., 2017, "Biofabrication and Bone Tissue Regeneration: Cell Source, Approaches, and Challenges," *Frontiers in Bioengineering and Biotechnology*, 5, p. 17, DOI: 10.3389/fbioe.2017.00017.
- [6] Lawrence, L. M., Salary, R., Miller, V., Valluri, A., Denning, K. L., Case-Perry, S., Abdelgaber, K., Smith, S., Claudio, P. P., and Day, J. B., 2023, "Osteoregenerative Potential of 3D-Printed Poly ϵ -Caprolactone Tissue Scaffolds In Vitro Using Minimally Manipulative Expansion of Primary Human Bone Marrow Stem Cells," *International Journal of Molecular Sciences*, 24(5), p. 4940, DOI: 10.3390/ijms24054940.
- [7] Li, B.-A., 2021, "Tasting Nuclear Pasta Made with Classical Molecular Dynamics Simulations," *Frontiers of Physics*, 16, pp. 1-3, DOI: 10.1007/s11467-020-1043-8.
- [8] Coburn, B., and Salary, R. R., "Computational Fluid Dynamics (CFD) Modeling of Material Transport through Triply Periodic Minimal Surface (TPMS) Scaffolds for Bone Tissue Engineering," *Journal of Biomechanical Engineering*, pp. 1-32, DOI: 10.1115/1.4067575.
- [9] Daver, A., "Scaffolds for Bone Using Inclined Schwarz TPMS; Design and Finite Element Analysis," Proc.

- International Science and Art Research Congress (ISARC), Istanbul, Turkey, 24-25 December 2022., p. 5, DOI: N/A.
- [10] Feng, J., Fu, J., Yao, X., and He, Y., 2022, "Triply Periodic Minimal Surface (TPMS) Porous Structures: From Multi-Scale Design, Precise Additive Manufacturing to Multidisciplinary Applications," *International Journal of Extreme Manufacturing*, 4(2), p. 022001, DOI: 10.1088/2631-7990/ac5be6.
- [11] Abdelgaber, Y., Klemstine, C., and Salary, R., 2023, "A Novel, Image-Based Method for Characterization of the Porosity of Additively Manufactured Bone Scaffolds With Complex Microstructures," *Journal of Manufacturing Science and Engineering*, 145(4), p. 041008, DOI: 10.1115/1.4056434.
- [12] Gerhardt, L.-C., and Boccaccini, A. R., 2010, "Bioactive Glass and Glass-Ceramic Scaffolds for Bone Tissue Engineering," *Materials*, 3(7), pp. 3867-3910, DOI: 10.3390/ma3073867.
- [13] Jiang, J., Huo, Y., Peng, X., Wu, C., Zhu, H., and Lyu, Y., 2024, "Design of Novel Triply Periodic Minimal Surface (TPMS) Bone Scaffold with Multi-Functional Pores: Lower Stress Shielding and Higher Mass Transport Capacity," *Frontiers in Bioengineering and Biotechnology*, 12, p. 1401899, DOI: 10.3389/fbioe.2024.1401899.
- [14] Depeng, G., Yuanzhi, Z., and Hongwei, L., 2024, "Persistent Homology-Driven Optimization of Effective Relative Density Range for Triply Periodic Minimal Surface," *arXiv preprint arXiv:2402.12109*, DOI: 10.48550/arXiv.2402.12109.
- [15] Homavand, A., Cree, D. E., and Wilson, L. D., "Polylactic Acid Composites Reinforced with Eggshell/CaCO₃ Filler Particles: A Review," *Proc. Waste, MDPI*, pp. 169-185, DOI: 10.3390/waste2020010.
- [16] Caplan, M. E., Schneider, A., and Horowitz, C. J., 2018, "Elasticity of Nuclear Pasta," *Physical review letters*, 121(13), p. 132701, DOI: 10.1103/PhysRevLett.121.132701.
- [17] Xia, C.-J., Maruyama, T., Yasutake, N., Tatsumi, T., and Zhang, Y.-X., 2021, "Nuclear Pasta Structures and Symmetry Energy," *Physical Review C*, 103(5), p. 055812, DOI: 10.1103/PhysRevC.103.055812.
- [18] "Phases of Nuclear Pasta 3D Models by Indiana University's Advanced Visualization Lab," <https://sketchfab.com/AVL>.
- [19] Mathieu, L. M., Mueller, T. L., Bourban, P.-E., Pioletti, D. P., Müller, R., and Manson, J.-A. E., 2006, "Architecture and Properties of Anisotropic Polymer Composite Scaffolds for Bone Tissue Engineering," *Biomaterials*, 27(6), pp. 905-916, DOI: 10.1016/j.biomaterials.2005.07.015.
- [20] Salary, R., 2022, "Perspective Chapter: Advanced Manufacturing for Bone Tissue Engineering and Regenerative Medicine," *Advanced Additive Manufacturing*, I. V. Shishkovsky, ed., IntechOpen, London, UK, p. 59, DOI: 10.5772/intechopen.102563.